Influence of interface roughness in quantum cascade lasers

Krivas, K. A.; Winge, David; Franckie, Martin; Wacker, Andreas

Published in:
Journal of Applied Physics

DOI:
10.1063/1.4930572

2015

Document Version:
Publisher's PDF, also known as Version of record

AIP Journal of Applied Physics

Influence of interface roughness in quantum cascade lasers

K. A. Krivas, D. O. Winge, M. Franckié, and A. Wacker

Citation: Journal of Applied Physics **118**, 114501 (2015); doi: 10.1063/1.4930572
View online: http://dx.doi.org/10.1063/1.4930572
View Table of Contents: http://scitation.aip.org/content/aip/journal/jap/118/11?ver=pdfcov
Published by the AIP Publishing

Influence of interface roughness in quantum cascade lasers

K. A. Krivas, D. O. Winge, M. Franckié, and A. Wacker[a)]
Division of Mathematical Physics, Lund University, Box 118, Lund 221 00, Sweden

(Received 18 June 2015; accepted 27 August 2015; published online 15 September 2015)

We use a numerical model based on non-equilibrium Green's functions to investigate the influence of interface roughness (IFR) scattering in terahertz quantum cascade lasers. We confirm that IFR is an important phenomenon that affects both current and gain. The simulations indicate that IFR causes a leakage current that transfers electrons from the upper to the lower laser state. In certain cases, this current can greatly reduce gain. In addition, individual interfaces and their impact on the renormalized single particle energies are studied and shown to give both blue- and red-shifts of the gain spectrum. © *2015 AIP Publishing LLC*. [http://dx.doi.org/10.1063/1.4930572]

I. INTRODUCTION

Quantum cascade lasers (QCLs)[1,2] have proven to be useful devices with important applications, as they can be designed to emit in the region of 5–14 μm, crucial to molecular spectroscopy.[3] These lasers are solid state devices that employ mini-bands to achieve population inversion and thereby lasing in semiconductor heterostructures. Due to their high possible wall-plug efficiency[4] and capability to operate in the mid-infrared (mid-IR) and terahertz regions of the electromagnetic spectrum that are poorly covered by other coherent radiation sources, these devices have attracted a lot of attention.

While mid-IR QCLs are already industrialized, possible applications[5] of THz QCLs are not reached due to a lack of room temperature operation. Difference frequency generation using mid-IR QCLs has proven to be a way, although with limited power.[6] In order to reach high temperature operation of THz QCLs, it is necessary to understand the underlying mechanisms that govern the operation of these devices.

The two main causes of elastic scattering in QCLs are impurities, where electrons are scattered by the dopant ions, and interface roughness (IFR), which provides scattering due to imperfections of the interfaces between two semiconductor layers. The interface roughness scattering[7,8] is dominant in mid-IR QCLs,[9] and is also relevant in THz QCLs.[10] It affects the occupation of states by scattering electrons from one mini-band into another, due to the lack of lateral symmetry at the interfaces. It was shown by Deutsch *et al.*,[11] by producing symmetrical lasers from materials, in which IFR depends on growth direction, that interface roughness scattering strongly affects the operation of THz QCLs.

Using our non-equilibrium Green's function (NEGF) model,[12] we investigate the influence of interface roughness in detail both with respect to growth direction and roughness fluctuations of individual interfaces. The use of a complicated and computationally expensive model is motivated by the access to several important features. Among these effects is the renormalization of the single particle energies from the scattering potentials. Thus, altering IFR can provide shifts of the energy levels. Furthermore, the approach is able to capture effects such as dispersive gain[13] and gain linewidth reductions due to correlations, which are crucial in THz QCLs.[14] These effects are unique to the NEGF scheme, thanks to the use of two times in the evaluation of the density matrix. A summary of different methods for modeling QCLs can be found in Ref. 15.

II. THEORY

In our numerical computation method documented in Ref. 12, the IFR scattering enters the equations through the self-energy, a physical quantity that describes the interaction of the particle with its surroundings. The real part of the self energy gives a shift in the energies of the single particle states, while the imaginary part is related to its lifetime.

IFR is characterized by the autocorrelation function for the spatial distributions of the deviation from a perfect interface. In this work, we chose an exponential autocorrelation function, given by

$$\langle f(\mathbf{r})f(\mathbf{r}')\rangle = \eta^2 \exp\left(-\frac{|\mathbf{r}-\mathbf{r}'|}{\lambda}\right). \tag{1}$$

The Fourier transform of this function is

$$f(q) = 2\pi \frac{\eta^2\lambda^2}{(1+(q\lambda)^2)^{3/2}}, \tag{2}$$

where q is the absolute change in wavevector, and the two variables λ and η describe the correlation length and root mean square deviation from a perfect interface, respectively.

A Gaussian distribution function is another common choice of autocorrelation function. However, as shown in Ref. 10, it is possible to obtain similar results by an appropriate transformation of parameters between both autocorrelation functions. Since there is no convincing physical argument for either of them, we normally use the exponential type.

In Fig. 1, we display Eq. (2) for the reference case and also for the case when η and λ are separately increased. It is possible to see that increasing the parameters λ and η have different effects on the scattering. While η increases the

a)Electronic mail: andreas.wacker@fysik.lu.se

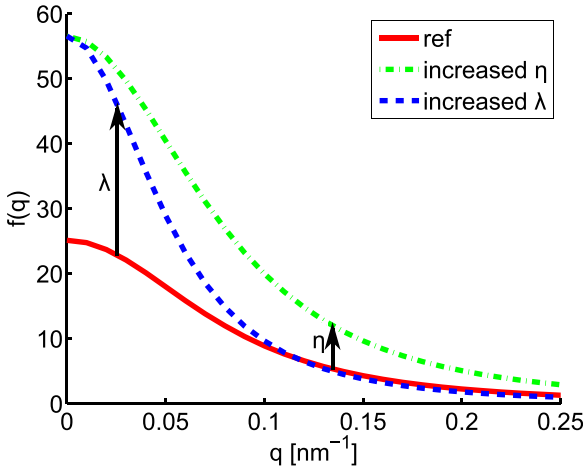

FIG. 1. Different forms of the autocorrelation function, Eq. (2). The full line is the reference case with $\eta = 0.20\,\text{nm}$ and $\lambda = 10.0\,\text{nm}$, the dashed line shows the case when λ is increased by 50% and the dotted-dashed shows the behavior for the same increase of η.

scattering over the entire range of q values, λ tends to emphasize low momentum transfer. Comparing results when these parameters are increased separately could give insight into how important scattering with large momentum transfer is.

As our non-equilibrium Green's function model applies the self-consistent Born approximation in the calculation of self-energies, multiple-scattering events with a single imperfection are neglected. Thus, we cannot reproduce any bound states due to disorder, which might cause distinct effects of inhomogeneous broadening. However, such effects only become of relevance for larger spatial correlation lengths as discussed in Section IV of Ref. 16. In order to quantify this, we consider the energy balance for localization at an island of size λ and thickness η. The possible gain in energy at an island with a locally enlarged well width is about $\eta\Delta E_c|\Psi(z_i)|^2$, where ΔE_c is the conduction band offset and $\Psi(z_i)$ the wave function at the interface. However, the lateral localization costs an energy larger than $\hbar^2/(m_c\lambda^2)$, where m_c is the effective mass. Thus, we can exclude any localization effects as long as

$$\lambda^2\eta < \frac{\hbar^2}{m_c\Delta E_c|\Psi(z_i)|^2}. \tag{3}$$

For all interfaces considered in this study, the right hand side is at least $100\,\text{nm}^3$ (for the thin barrier in the four-well laser). Thus, the inequality holds even for the enlarged values $\lambda = 15\,\text{nm}$ and $\eta = 0.3\,\text{nm}$.

An alternative approach to study these issues is the use of exact eigenstates.[7] We could actually show that the lineshape of our model agrees with such calculations very well,[17] which justifies the Born approximation for interface roughness.

III. DEVICES STUDIED

In this work, the influence of IFR scattering is investigated using three different terahertz QCL designs, namely, a two-well,[18] a three-well,[19] and a four-well[20] structure. The first one employs three states per period for electron transport: an upper lasing state (ULS), a lower lasing state (LLS), and an injector-extractor state (i-e), as shown in Fig. 2. This laser operates over a range of frequencies from 2.8 to 4.1 THz, with a maximum reported operating temperature of 125 K. The second (three-well) laser is of resonant phonon design and therefore has separate states for injection (i) and extraction (e). The reported lasing frequency is 3.9 THz, and the reported maximum temperature of operation is 186 K. The band diagram of this laser is displayed in Fig. 3. The last investigated QCL employs a scattering assisted design. It relies on 4 mini-bands distributed over four wells per period. This laser operates at 3.2 THz at the maximum temperature of 138 K. The band diagram is shown in Fig. 4.

IV. RESULTS

We investigate the influence of IFR scattering by altering the interface roughness parameters in the simulations. These results are then compared to simulations with unaltered IFR. As a reference, we use the parameters $\lambda = 10\,\text{nm}$ and $\eta = 0.20\,\text{nm}$. The IFR of the altered interfaces is chosen to have one of these two parameters increased by 50%. The interfaces are also assumed to be uncorrelated, so that one interface distribution does not depend on the others.[21] All simulations are performed for a lattice temperature of 200 K.

It is known that interface roughness can depend on growth direction.[11] Therefore, increasing IFR on every second interface would recreate the naturally occurring configuration. The applied bias tilts the potential wells and lets us distinguish between two different cases: first, when the altered interfaces are on the lower potential side of the wells (*wb*), and second, when the altered interfaces are on the higher potential side of the wells (*bw*).

First, we investigate the effect of IFR scattering on the current density. The results when either half of the interfaces or all of them are altered are shown in Fig. 5. If the changes

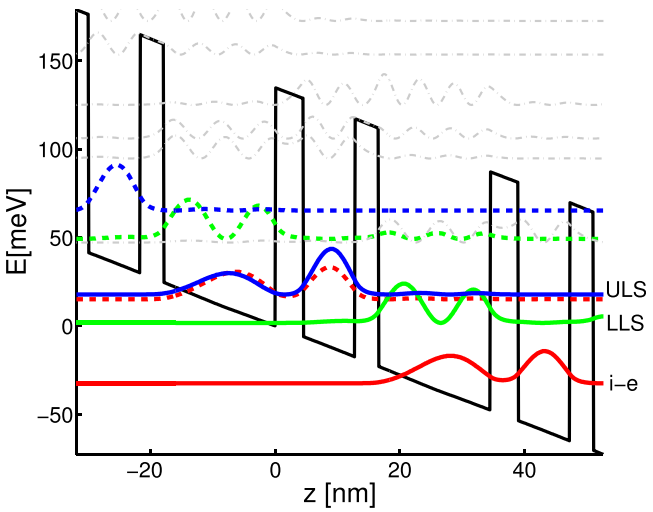

FIG. 2. Band diagram of the two-well laser[18] at 47.5 mV per period with respect to the growth direction z. The conduction band profile is shown together with the probability density for the most important subbands at their respective energies.

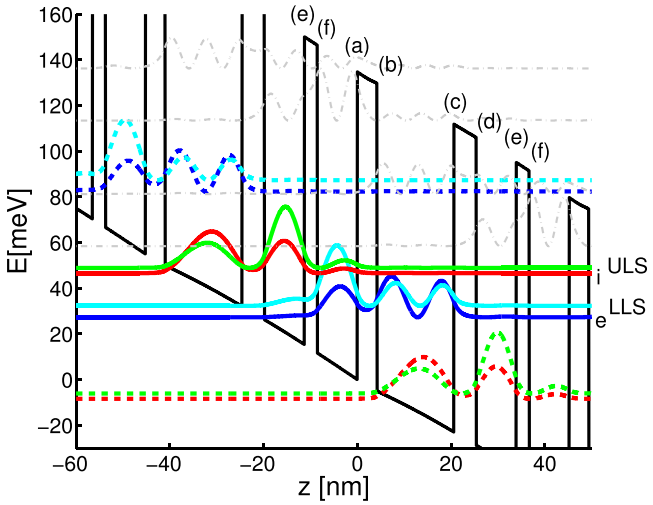

FIG. 3. Band diagram of the three-well laser,[19] in the same way as Fig. 2 with labels added to distinguish the specific interfaces. The bias is 55 mV per period.

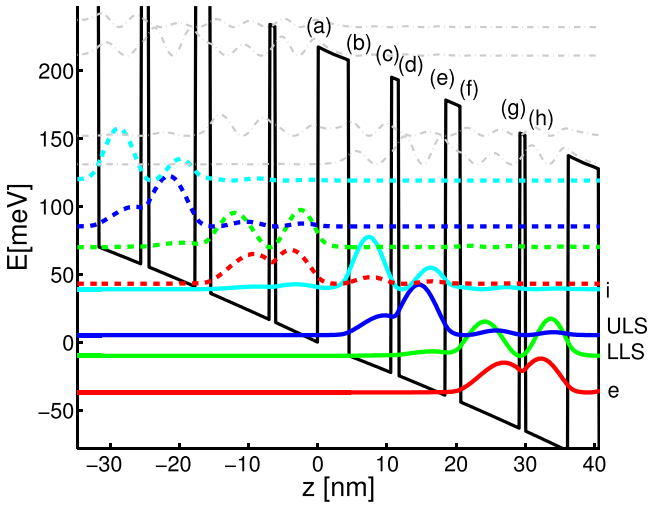

FIG. 4. Band diagram of the four-well laser[20] plotted in the same way as in Fig. 3, at a bias of 80 mV per period.

in current due to a change in IFR are small, we expect that if we increase the interface roughness on two interfaces simultaneously, we obtain the same change in current density as if we would add the changes in current densities from simulations when these two interfaces have roughness increased separately. As can be seen from Fig. 5, it is actually possible to relate the magnitude of the increase in current density to how well this superposition holds. For instance, the two-well laser exhibits the lowest increase in current (4%) and shows the best agreement between simulated relative current and the sum, while the four-well laser shows the least agreement, and the increase in current is the highest (21%). The three-well laser is an intermediate case, having 11% increase in current density when η is increased by 50% on all interfaces.

It can be seen in Fig. 5 that altering *wb* interfaces causes a larger increase in current density than *bw* interfaces. This can be understood by the effect that the wavefunctions tend to shift to the lower potential side of the well when a bias is applied, as can be seen in Figs. 2–4. This results in higher wavefunction values at the interfaces at the lower potential side of a well. Since IFR scattering is proportional to the product of the wavefunction values at the interfaces, changing IFR on interfaces with high wavefunction values has a larger impact on the transport. This observation confirms the results shown in Ref. 11.

For the two- and three-well lasers, the results of Fig. 5 can be understood using the reasoning above. Here, the (*wb*) interfaces dominates the IFR scattering. However, in the four-well case, the changes due to *wb* and *bw* are approximately the same. This is an effect of the thin barriers, as the value of the wavefunction of the ground state is actually lower on the high potential side of the barrier (or, equivalently, on the low potential side of the foregoing well) as seen in Fig. 4. This is because thin barriers are placed where the ground state wavefunctions have their maximum, rather than their minimum, value. However, the thick barriers act as in the cases of the other two lasers.

The simulated relative gain spectra compared to unaltered IFR, for the respective devices are shown in Fig. 6, and all devices show an overall decrease in gain as a result of increasing IFR. However, the magnitude of the effect differs widely. Again, the two-well laser is the most insensitive to changes in IFR, with a decrease in gain of 7.2%. The three-well laser displays a 19.1% reduction, while the gain of the four-well laser shows a decrease by 50.6% when roughness parameter η was increased by 50% on all interfaces.

In order to determine in detail the influence of individual interfaces on the current density and gain, we now change only one interface at a time and compare these results to the reference case. These results are shown in Fig. 7 for the three-well laser. The effects of the changes are twofold; we

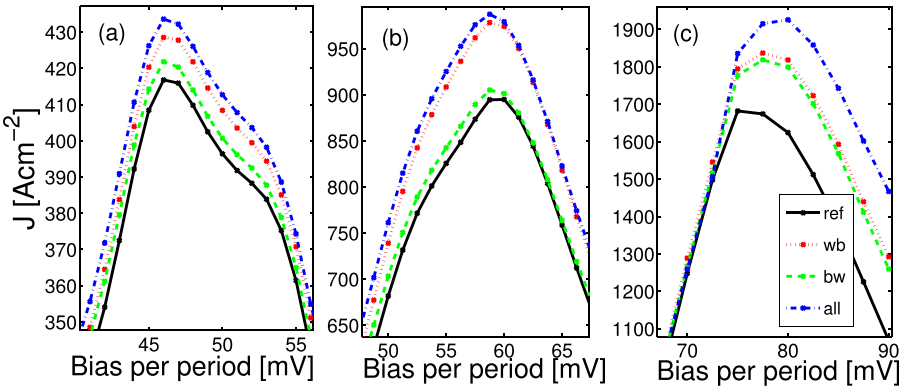

FIG. 5. Results of current density simulations. (a) Two-well laser,[18] (b) three-well laser,[19] and (c) four-well laser.[20] The parameter η is increased by 50% with respect to the reference calculation (ref) for different sets of interfaces.

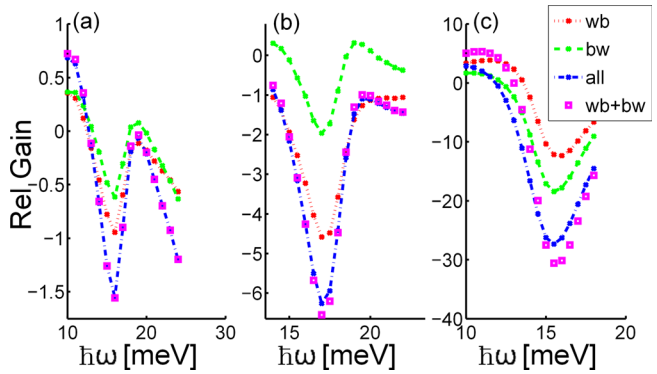

FIG. 6. Relative gain at operation bias *per period*. In (a), the two-well laser[18] at 47.5 mV, (b) the three-well laser[19] at 55 mV, and (c) four-well laser[20] at 80 mV. In this study, η is increased.

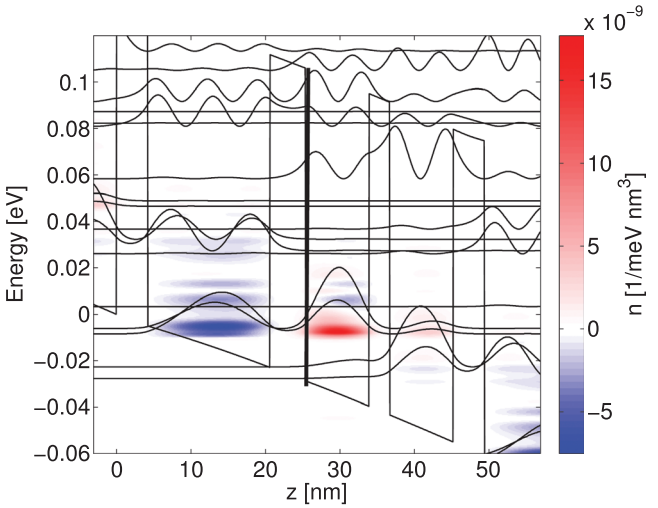

FIG. 8. Changes in spatially and energetically resolved charge density due to increase of η on one interface (marked by black line). This configuration results in shift in gain as shown in Fig. 7(d). Results for the three-well laser for a bias of 57.5 mV per period.

see both reductions and shifts in the gain spectra. There is an overall decrease in magnitude due to the enhanced depopulation of the ULS, being the main effect in (a) and (e). This is also reflected in the significant increase in current. These two are *wb* interfaces and, following the above discussion, crucial to the operation. In contrast, the main effect in (b), (c), and (f), is a blue-shift. As the scattering potential is increased, there will be a renormalization of the single particle energies. In our model, this is taken into account by the real part of the self energies, but it can be understood in general as a level shift in second order perturbation theory. The intraband scattering will shift the levels down in energy, and for the interfaces (b), (c), and (f), this effectively lowers the LLS, which gives a blue-shift. This interpretation is strengthened by the remaining case, Fig. 7(d) where the ULS is mostly affected. Here, in combination with a gain reduction, a red-shift is observed. In all cases, the impact of changing η and λ is similar, albeit λ has less impact due to the limited strength at higher q-values.

One of the possible causes for changes in gain and current density might be a leakage into high kinetic energy states of lower energy mini-bands. This leakage can be observed by investigating the change in spatially and energetically resolved electron densities. The change in electron density for the simulation of Fig. 7(d), shown in Fig. 8, shows an increase in the occupation near the bottom of the ULS. Thus, in accordance with Fig. 7(d), this is not expected to result in a significant decrease in gain. In contrast, the change in densities shown in Fig. 9, which correspond to Fig. 7(e), shows an increase in charge density at higher energies in the LLS. This indicates that electrons are scattered elastically and then relaxes by optical and acoustic phonon scattering. This lowers the inversion between the ULS and LLS, and consequently reduces the gain.

Comparing the values in Fig. 7, one finds that interfaces at the lower side of the well affect gain more, in agreement with the results from the current density simulations. Large decreases in gain are observed at the interfaces where the ULS and LLS have high wavefunction values.

For the case of the four-well QCL, shown in Fig. 4, the thicker barriers affect gain similarly to the other structures. However, the effect of the interfaces of the thin barriers is dominating the reduction in gain, as displayed in Fig. 10. For

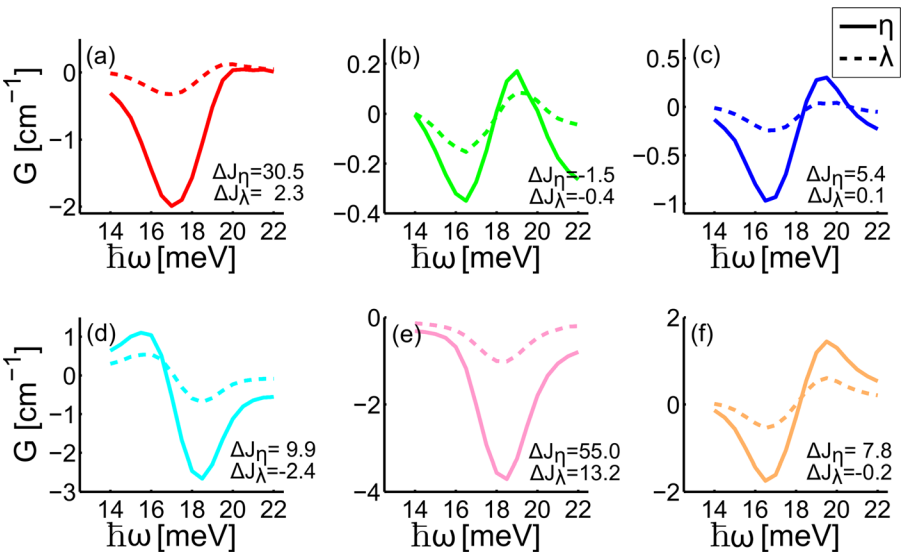

FIG. 7. Changes (relative gain) due to alteration of a single interface in each period of the three-well laser.[19] Also included are the changes in current in units of A/cm^2. The respective interfaces are denoted in Fig. 3. Either η or λ were increased by 50%. The bias is 57.5 mV per period.

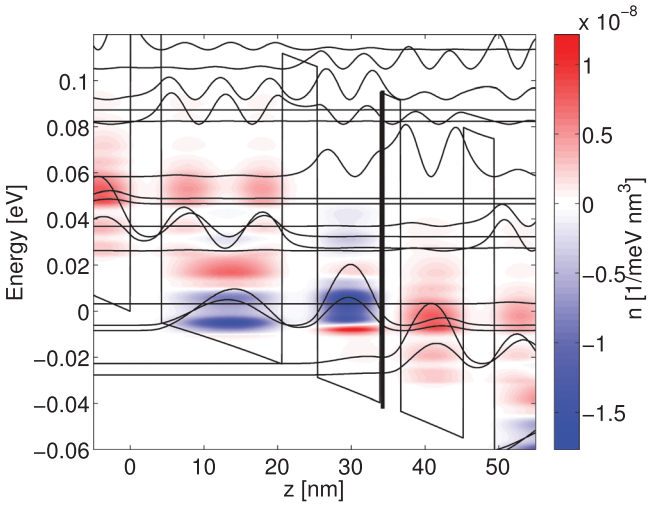

FIG. 9. Changes in spatially and energetically resolved charge density due to increase of η on one interface (marked by black line). Simulation shows strong reduction in gain as shown in Fig. 7(e). Results for the three-well laser for a bias of 57.5 mV per period.

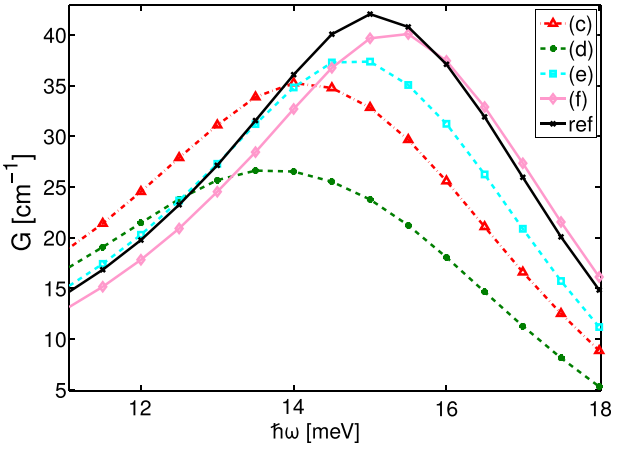

FIG. 10. Gain spectrum of the four-well laser. η is increased on the indicated interfaces, as labeled in Fig. 4, by 50%. Only the most important interfaces are shown for clarity.

these barriers, the aforementioned rule, that the (*wb*) interfaces are the most important, does not hold. This can be understood by examining the probability density of the ULS in Fig. 4. Here, it is clear that it has a larger value at interface (d) compared to (c).

V. CONCLUSION

In this work, we numerically investigate the influence of interface roughness on the operation of several THz QCL designs. We confirm that IFR scattering is an important phenomenon that may greatly affect both current density and gain. The most sensitive interfaces are the ones, where the wavefunctions have significant values. This makes interfaces at the lower potential side of wells more important than those on the side of higher potential. Thin barriers work differently, impacting transport and gain significantly more since they are usually placed where the ground state wavefunctions have their maximum values. Increased current and decreased gain indicate that a certain leakage current forms at the interfaces. At certain interfaces, this leakage mechanism strongly reduces population inversion. Due to alterations in the scattering potential, a shift of the gain peak frequency is observed for some interfaces. This can be explained by changes in the real parts of the self-energy.

ACKNOWLEDGMENTS

The research leading to these results has received funding from the European Union Seventh Framework Programme (FP7/2007–2013) under Grant Agreement No. 317884, the collaborative Integrated Project MIRIFISENS and the Swedish Research Council (VR).

[1]J. Faist, F. Capasso, D. L. Sivco, C. Sirtori, A. L. Hutchinson, and A. Y. Cho, Science **264**, 553 (1994).
[2]J. Faist, *Quantum Cascade Lasers* (Oxford University Press, Oxford, 2013).
[3]R. F. Curl, F. Capasso, C. Gmachl, A. A. Kosterev, B. McManus, R. Lewicki, M. Pusharsky, G. Wysocki, and F. K. Tittel, Chem. Phys. Lett. **487**, 1 (2010).
[4]Y. Bai, N. Bandyopadhyay, S. Tsao, S. Slivken, and M. Razeghi, Appl. Phys. Lett. **98**, 181102 (2011).
[5]B. S. Williams, Nat. Photonics **1**, 517 (2007).
[6]M. A. Belkin, F. Capasso, F. Xie, A. Belyanin, M. Fischer, A. Wittmann, and J. Faist, Appl. Phys. Lett. **92**, 201101 (2008).
[7]J. B. Khurgin, Appl. Phys. Lett. **93**, 091104 (2008).
[8]Y. Chiu, Y. Dikmelik, P. Q. Liu, N. L. Aung, J. B. Khurgin, and C. F. Gmachl, Appl. Phys. Lett. **101**, 171117 (2012).
[9]Y. V. Flores, S. S. Kurlov, M. Elagin, M. P. Semtsiv, and W. T. Masselink, Appl. Phys. Lett. **103**, 161102 (2013).
[10]M. Franckié, D. O. Winge, J. Wolf, V. Liverini, E. Dupont, V. Trinité, J. Faist, and A. Wacker, Opt. Express **23**, 5201 (2015).
[11]C. Deutsch, H. Detz, T. Zederbauer, A. M. Andrews, P. Klang, T. Kubis, G. Klimeck, M. E. Schuster, W. Schrenk, G. Strasser, and K. Unterrainer, Opt. Express **21**, 7209 (2013).
[12]A. Wacker, M. Lindskog, and D. O. Winge, IEEE J. Sel. Top. Quantum Electron. **19**, 1200611 (2013).
[13]A. Wacker, Nat. Phys. **3**, 298 (2007).
[14]F. Banit, S.-C. Lee, A. Knorr, and A. Wacker, Appl. Phys. Lett. **86**, 041108 (2005).
[15]C. Jirauschek and T. Kubis, Appl. Phys. Rev. **1**, 011307 (2014).
[16]T. Unuma, M. Yoshita, T. Noda, H. Sakaki, and H. Akiyama, J. Appl. Phys. **93**, 1586 (2003).
[17]C. Ndebeka-Bandou, F. Carosella, R. Ferreira, A. Wacker, and G. Bastard, Appl. Phys. Lett. **101**, 191104 (2012).
[18]G. Scalari, M. I. Amanti, C. Walther, R. Terazzi, M. Beck, and J. Faist, Opt. Express **18**, 8043 (2010).
[19]S. Kumar, Q. Hu, and J. L. Reno, Appl. Phys. Lett. **94**, 131105 (2009).
[20]E. Dupont, S. Fathololoumi, Z. R. Wasilewski, G. Aers, S. R. Laframboise, M. Lindskog, S. G. Razavipour, A. Wacker, D. Ban, and H. C. Liu, J. Appl. Phys. **111**, 073111 (2012).
[21]S. Tsujino, A. Borak, E. Muller, M. Scheinert, C. Falub, H. Sigg, D. Grutzmacher, M. Giovannini, and J. Faist, Appl. Phys. Lett. **86**, 062113 (2005).